Magnetic Resonance Imaging (MRI) Theory and Imaging Techniques: A Technical Mini-Review

Wasiu A. Balogun, Momoh-Jimoh E. Salami, Abiodun M. Aibinu, Adesanya Gbenga, Keshinro K..K.

Abstract— This paper takes care of the theoretical underpinnings of Magnetic Resonance Imaging (MRI) and stated the mathematical model that governed the principle development of MRI. We discussed the experimental data steps as well as design analyses that are related to MRI image development. The Instrumentation composition of MRI machine mainly used for farm fruits and vegetables research work were described in detail and shows each stage of processing mode. We finally suggested the possibility of developing on-spot assessment of farm produce internal quality using portable MRI couple with the robot or unmanned aerial vehicle (UAV) as the future research focus to deal with some of the limitations.

Index Terms— Magnetic Resonance Imaging, Fourier Transform, Radio Frequency, Resonance, K-space, Fruits and vegetables

1. Introduction

THE developments of various methods for quality determinant factors have been encouraged during recent years and few of these methods are non-destructive while large percentage falls in the category of destructive methods. The level of technology awareness has increased the appetite to develop methods that are not destructive.

The commonly used methods have only been able to grade farm produce using external features, which are sometimes at variant with the internal structure of the farm produces thus affecting the quality of the extract. There are numerous non-destructive techniques (NDT) such as X-ray, ultrasonic, vibrated excitation, sonic, impedance, CT, near infra-red (NIR) and ultra-violet that are available for determining internal quality of fruits and vegetables. Many of them have been applied to determine internal qualities of farm produces, though all these methods currently in use have their disadvantages or deficiencies. More so, with improvement in technology, the capability of obtaining cross-sectional images in any desired direction, high resolution, diffusion imaging, flow-related imaging and ability to use a variety of high tissue contrast in MRI is very possible.

- *Balogun Wasiu Adebayo, MIEEE, MSc. Mechatronics Engineering and currently working towards his PhD in Engineering. A Research Scholar with University of California Davis USA and presently a Senior lecturer with Lagos State Polytechnic Ikorodu Dept. of Mechatronics Engineering balogun.w1@mylaspotech.edu.ng*
- *Co-Author1: Momoh-Jimoh E. Salami a Professor in Mechatronics Engineering Dept., International Islamic University Gombak, 53100 Malaysia Email: momoh@iium.edu.*
- *Co-Author 2: Abiodun M Aibunu is a Professor in the Dept. of Mechatronics Engineering, Federal University of Technology Minna Niger State Nigeria. E-mail: maibunu@gmail.com*
- *Co-Author 3: Gbenga Adesanya* Bsc. Mechatronics Engineering and *presently a Lect*urer with Lagos State Polytechnic Ikorodu *Dept. of Mechatronics Engineering E-mail:gbengaadesanya25@yahoo.com*
- *Co-Author 4: Keshinro K.K. a Senior Lect*urer with Lagos State Polytechnic Ikorodu *Dept. of Computer Engineering*

Grading of farm produces qualities in the past decade have since turned out to be well mechanized, particularly with the application of robotics and mechatronics expertise, though majority such research works concentrated more on external quality assessment than internal (Kondo, [1]). Similarly, (Du & Sun, [2]) repeated that grading of fruit is essentially based on external quality evaluation which is commonly used and internal quality grading which is seldomly applied.

The commencement of procedure in determining the internal quality of farm produces is becoming a principal challenge in recent time. Most of the procedure currently used to assess farm produces works in an invasive form, hence, non-destructive quality assessment of farm produces is becoming necessary for agricultural and food manufacturing (Du & Sun, [2], Kleynen et al [3]).

However, researchers are focusing on usage of MRI for fruits and vegetables quality in recent time. MRI is an imaging technique that utilizes the magnetic properties of nuclei in relation with radio frequency and magnetic field. It is sensitive to the local environment of water and oil which are important composition of farm produce. Therefore, a system without any of the mentioned deficiencies necessitates the application of MRI. (Ebrahimnejad, H et al [4], Lu Zhang et al [5]).

Furthermore, MRI is used to acquire two and three-dimensional images of biological systems from obscured materials. It has been used to predicts the tomato maturity with PLS-DA model for classification and shows that different maturity stages are embedded in MR images signal intensity (Zhang & McCarthy, 2012). Since 1973, medical expert has commonly been applying magnetic resonance imaging (MRI) for diseases diagnosis to determine internal defect (Bhaiya et al [6] Pekar [7]).

Table 1
Nobel Prizes on MRI and NMR (Euclid Seeram [8]

Name and year	Contribution
Otto Stern, 1888-1969, Prize 1943	For his role to the advancement of the molecular ray method and finding of the magnetic moment of the proton
Isidor I. Rabi, 1898-1988, Prize 1944 in physics	For his resonance technique for recording the magnetic properties of atomic nuclei"
Felix Bloch, 1905-1983, and Edward M.Purcell, 1912-1997, Prize 1952	For the advancement of new techniques for nuclear magnetic precision measurements and discoveries in association therewith
Nicolaas Bloembergen, 1920-, Prize 1981 in physics	For his role to the contributions of laser spectroscopy" (Theory of NMR relaxation)
Richard Ernst, 1933-, Prize 1991 in chemistry	For his development to the contributions of the methodology of high resolution nuclear magnetic resonance (NMR) spectroscopy" (Pulsed techniques and Fourier transform methods)
Kurt Wütrich, 1938-, Prize 2002 in chemistry	For his contributions on nuclear magnetic resonance spectroscopy for determining the three-dimensional structure of biological macromolecules in solution
Paul C. Lauterbur, 1929-, and Sir Peter Mansfield, 1933-, Prize 2003 in physiology or medicine	For their finding concerning magnetic resonance imaging

2 MRI Theory

2.1 Basic

Nuclear magnetic resonance (NMR) is atomic nuclei occurrence that possesses magnetic properties Fig 1. NMR happen through a physical property of protons and neutrons identified as spin which occurred in two forms positive or negative (Nishimura [9]). It is essential to recognize that protons and neutrons tend to group themselves in spin and opposed pairs which cancel out the effects of spin in many atoms. Most Magnetic Resonance (MR) active nuclei that comprised of an odd number of proton and neutron, possess spin. element are ^{1}H, ^{13}C, ^{14}N, ^{17}O, ^{19}F, ^{23}Na.

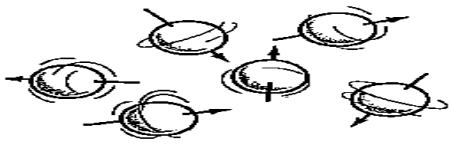

Figure 1: Macroscopic magnetization of tissue

$$\omega_o=\gamma B_0 \quad (1)$$

When this spin is put in a magnetic field (B_o) (Figure 1), nuclei experience a torque which tends to align them with the field direction or against the magnetic field (B_o) at the Larmor frequency (ω_o) as in "(1),"known as Larmor equation (Hashemi et al [10], Hornak [11], Nishimura [9])

Where ω_o is angular precessional frequency of proton γ is a constant called gyromagnetic ratio specific to each species of magnetic nuclei and β_o is the external magnetic field strength. For instance the gyromagnetic ratio of a proton is about 42.86MHz/Tesla, and if resonance frequencies of protons are 64.29, 85.72 and 257.16 MHz then 1.5, 2.0 and 6 Tesla magnetic fields strength are obtained respectively (Nishimura [9])

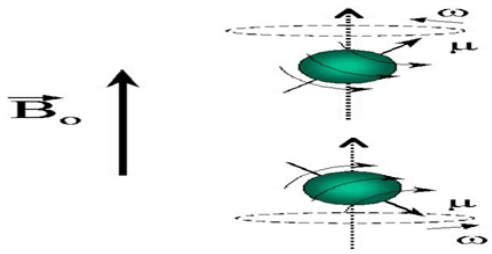

Figure 2: Particle precessing around an external magnetic field (B_0)

.

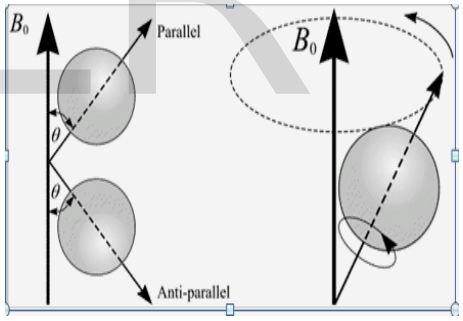

Figure 3: After application of external magnetic field B_o only two energy states are allowed parallel or anti-parallel to B_o

There will be a net magnetic moment M_o resulting from the sum of all nuclei aligning along B_o (Figure 3). Once a secondary oscillating radiofrequency (RF) pulse magnetic field with amplitude B_1 and frequency ω_o perpendicular to B_o is applied, the net magnetization M_o will be disturbed by an angle θ. The angle θ is proportional to the magnitude of B_o as well as the duration of acting of B_o. This process mean that since each species of nucleus precesses at its own frequency, oscillating the B_o field at the same rate will result in resonance.(Talagala et al [12], Yang et al[13[)

After an RF pulse the magnetization M_o will reverse to its equilibrium state which is along static magnetic field B_o and this procedure of going back to equilibrium state is referred to as relaxation. The signal from the magnetization free induction

decay (FID) is recorded by the receiving system. Relaxation time and chemical shift are important variables for magnetic resonance imaging. For the same nuclear species for example ^1H in different chemical bond, ^1H is in a different local magnetic environment therefore the Larmor frequency is slightly different. Chemical shift of a peak in the spectrum is defined as the relative difference of Larmor frequency from a reference peak in parts per million (p.p.m) units as stated in "(2),"

$$\delta = (v - v\_ref)/v\_ref \quad 〚10〛 \hat{}6 \ p.p.m \tag{2}$$

where v is the resonant frequencies of the spectral peak of interest and v_{ref} is the resonant frequencies of the spectral peak of the reference component. Whereas the effect of chemical shift is expressed in "(3),"

$$B = (1 - \sigma)B_0 \tag{3}$$

σ stand for shielding constant and "(3)," above adjust the Larmor frequency in "(4),"

$$\omega = \gamma(1 - \sigma)B_0 \tag{4}$$

When a resonant RF pulse is applied to disturb the spin system from equilibrium state the net magnetization will try to go back to the equilibrium state by the process of spin-lattice relaxation which involves the energy exchange between the spin-system itself. The relaxation behaviour is governed by Bloch equation with the spin-lattice relaxation process in rotating frame (Hinshaw & Lent [14], Yang et al [13]) described by the either "(5),"or "(6),"

$$dM/dt = \gamma MH - (\ 〚(M〛 \_x \ i + M\_y \ j))/T\_2 \ - (M\_2 \\ - M\_0 \ )k/T\_1 \tag{5}$$

$$(\ 〚dM〛 \_z \ (t))/dt \ = \ - (M\_(z\hat{}((t)) \ ) - M\_o)/T\_1 \tag{6}$$

With solution

$$M\_z \ (t) = \ M\_z \ (0) \ e\hat{}((-t) \ / \ T\_1 \ ) + \\ M\_o \ (1 - e\hat{}((-t) \ / \ T\_1 \ )) \tag{7}$$

Where M_z is the component of magnetization in z direction (along B_o), $M_{z(0)}$ is the magnetization at equilibrium state, t is delay time right after excitation . T_1 is the longitudinal relaxation time which is as well refers to as spin-lattice relaxation time.

The spin-echo relaxation process can be described by the "(8),"

$$(\ 〚dM〛 \_(x,y) \ (t))/dt = (\ 〚- M〛 \_(x,y \ ) \ (t))/T\_2 \tag{8}$$

Which result to

$$M\_(x,y) \ (t) = M\_(x,y) \ (0)e\hat{}((-t) \ / \ T\_2 \ ) \tag{9}$$

Where $M_{x,y}$ is the component of magnetization on xy plane which is perpendicular to B_0 and T_2 is the transverse relaxation time also refers to as spin-spin relaxation time.

Inversion-recovery pulse sequence can be applied to determine T_1. The pulse sequence is shown in (Figure 4) both 180^0 and 90^0 are non-selective pulse and the signal is obtained after the 90^0 pulse. Spin-echo pulse can be used to determine T_2 with the pulse sequence in Figure 3 with both 180^0 and 90^0 are non-selective and the signal is acquired after the 180^0 pulse.

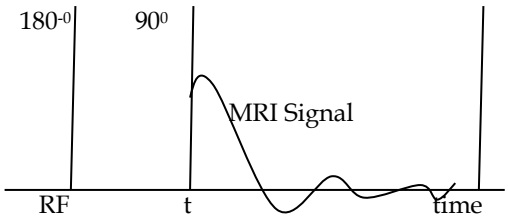

Figure 4: Inversion-recovery pulse sequence for measuring T_1

Figure 5: Spin-echo pulse sequence for determining T_2. The signal

Magnetic resonance imaging is accomplished by applying magnetic field gradients usually linear field gradients. Two types of RF pulse that are available namely soft pulse also known as selective pulse and hard pulse also referred to non-selective pulse. Soft pulse excites only the spins with a certain frequency range whereas hard pulse excites all the spins in the sample. When magnetic gradient is applied the Larmor frequency becomes a function of position since Larmor frequency is proportional to the magnetic field experienced by the nuclei. (Hashemi et al.[10], Talagala & Lowe [12], Zhang & McCarthy [15])

After the free induction decay (FID) signal is collected in the presence of a gradient and Fourier transformed, the position information is revealed. This is called frequency encoding. Since field gradient causes nuclei to precess at different Lar-

mor frequency, after some time of precession they have different phase. The phase of signal can be related to lessen the effect of eddy current caused by RF pulse and switch of gradient and to reduce the effect of magnetic field inhomogenity. Difference of relaxation time, chemical shift and spin density can be used in magnetic resonance imaging.

A spin-wrap imaging sequence commonly referred to 2DFT as described by (Edelstein et al [16]) can be used to do T_1 and /or T_2 weighted contrast imaging. The pulse sequence is shown in (Figure 6).

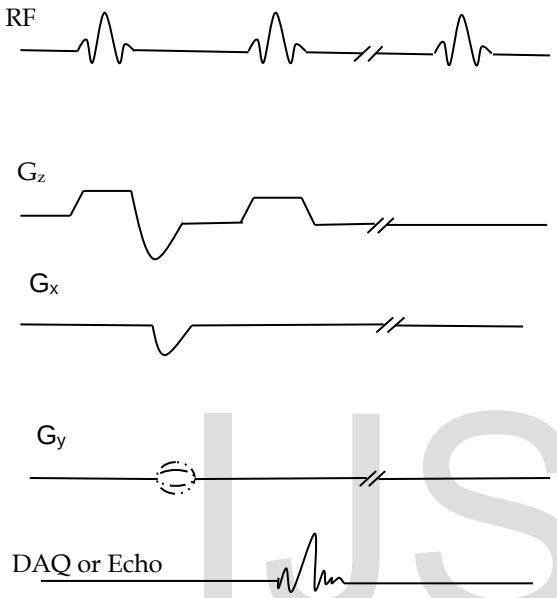

Figure 6: Spin-wrap imaging pulse sequence

Both 90^0 and 180^0 are selective pulse with 180^0 for spin echo purpose, G_x is readout gradient, G_y is phase encode gradient, G_z is slice selective gradient and DAQ or echo is data acquisition.(Hashemi et al [10], Westbrook & Roth [17])

The signal intensity is determined by T_1, T_2 tip angle, echo time, repetition time and the spin density. If the tip angle is 90^0, the signal amplitude from a spin-echo can be expressed as

$$M_y = M_0\left[1 - 2e^{\frac{-T_R+\frac{T_E}{2}}{2}} + e^{\frac{T_R}{T_1}}\right]e^{\frac{-T_E}{T_2}} \quad (9)$$

The signal intensity is determined by T_1, T_2 tip angle, echo time, repetition time and the spin density. If the tip angle is 90^0, the signal

amplitude from a spin-echo are stated as in "(10),"

$$M_y = M_0[1 - 2e^{\frac{-T_R+\frac{T_E}{2}}{2}} + e^{\frac{T_R}{T_1}}]e^{\frac{-T_E}{T_2}} \quad (10)$$

Where M_0 is the magnetization in equilibrium state, T_R is repetition time, T_E is echo time. If samples have differences in T_1 normally short repetition time and short echo time are used to get T_1 weighted contrast image. It is also possible to choose appropriate repetition time and echo time to get a good contrast if both T_1 and T_2 different. If the samples have different M_0 resulting from spin density it is possible to get spin density contrast image. If a very narrow bandwidth RF pulse is used to selectively excite the nuclei that have special chemical shift, only the specified chemicals are excited give signals and are imaged. Diamagnetic susceptibility can also be used in MRI to get good contrast (Li T.-Q et al [18], Westbrook & Roth [17]).

2.2 Fourier transform and K-space

Out of the different methods presently in style for spectral evaluation, the conventional Fourier transform technique is the applicable type. K-space is derived from the data space which corresponds to the two to three dimensions spatial frequency information. Due to the oscillating nature of the signals, the image of the data space will appear as a series of concentric rings of signal intensity with alternating bands of high and low intensity as the signal oscillates from maximum to minimum but an overall decrease in intensity as one goes from centre to periphery. So the dark and white rings in the k-space correspond to the valleys and peaks of the echoes respectively (Figure 9).

The Fourier transform (FT) of k- space gives two main component of data space as real and imaginary components. FT shows correlation between image data and k-space data (Figure 10). As a result of varying the gradient of a period of time through Fourier space, the k-space data are sampled in a trajectory. K-space is where we store our MR signals. The data we collect in MRI is the same data you find in what is referred to as k-space. It is simply an array of numbers, but because those numbers represent a certain type of data, that array has a number of interesting properties. An array with those properties is called k-space.

The most essential data is found in the centre of k-space and it is just an array of complex numbers, which is why we can assign grey-scale values to those numbers and plot k-space like an image. Therefore k-space is a data space with each line depicting a sampled version of the received signal that is the echo. The coordinates in data space are in time with the vertical scale in the order of TR and the horizontal scale in the order of the sampling interval.

Thus because the phase is never zero, therefore the real and imaginary image are combined to obtain a composite image, which is the display MR image "(11),". The MR image is the combined data corresponding to the Fourier transform of the real and imaginary data space as in (Figure 7).

Data point = image = $\sqrt{(\text{Real image}^2+\text{Imaginary image}^2)}$.
plotted (11)

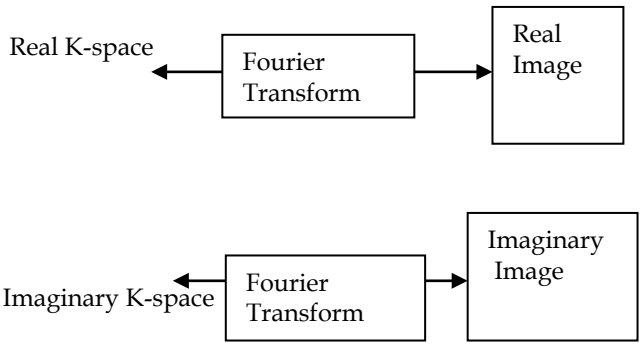

Figure 7: The Fourier transform (FTs) of the real and imaginary K-space give the real and imaginary images.

(From Figure 8) the magnitude image is what we consider in this work although this is what usually consider compared to phase image which is applicable when direction is important as in the case of Magnetic resonance angiography where the phase shows the direction of flow.

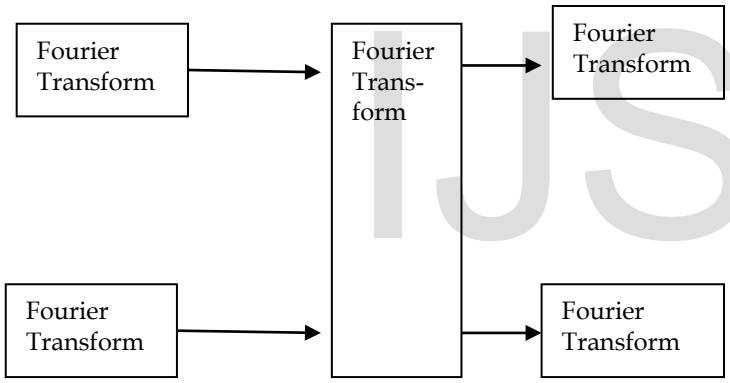

I_a

Figure 8: Real and imaginary images I_a are employed to construct magnitude and phase images I_b

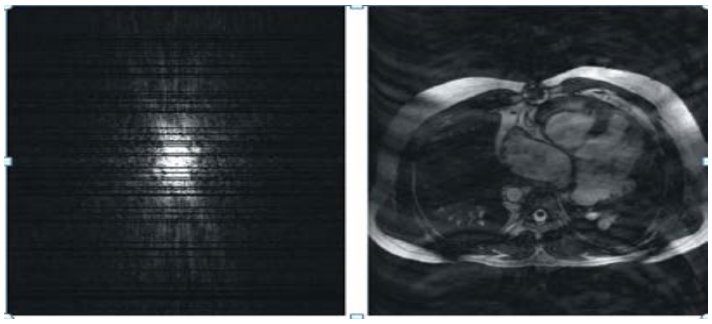

A B

Figure 9: (A) the original raw data (k-space) of (B) the original image (Biomedical Imaging and Intervention Journal)

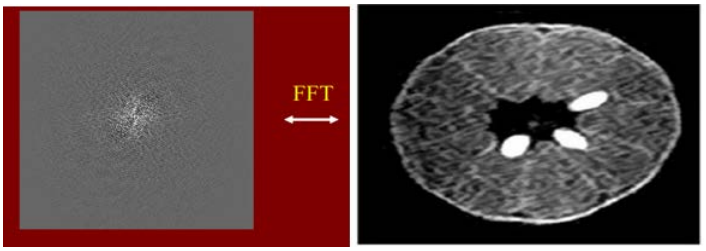

The k-space as measured in the MRI equipment

The Image is the Fourier transform of K-Space

Figure 10: MRI Fast Fourier Transform (FFT)

2.3 2D and 3D imaging

In 2D MR imaging, a single slice is excited at a time. The slices are adjacent and, ideally, have no gaps between them. The field of view (FOV) of each slice is rectangular and approximately 2–3 mm in thickness. In 3D MR imaging, the entire object is excited as a volume. The TR values for 2D imaging are usually between 200 and 300 ms. The ideal flip angle is between 70○ and 90○.

The 3D acquisition technique allows thin slices to be acquired with no gaps (typically 2mm thick). Another advantage of the 3D acquisition technique is a shorter acquisition time. This is the result of the shorter repetition time (TR) that is usually in the order of10 ms. The flip angle for 3D imaging is typically 25. However, 3D MRI acquisition suffers from a higher susceptibility to artefacts and requires a higher dose of contrast agent.

Fast Fourier Transform (FFT): Conventionally, MRI is a Fourier transforms based method. Frequency or phase encoding is always carried out and the data obtained are kept in a line K-space, during data acquisition. Fast Fourier Transform (FFT) technique is applied to convert the collected data in K-space to an image which is done by converting signal intensity in time domain to signal intensity in frequency domain, mathematically. It is also known as inverse Fourier transform (Aibinu et al [19], Hashemi et al [10], Westbrook & Roth [17])

2.4 Magnetic Resonance Imaging System Description

The M2 MRI system used for this work is a compact, high-performance MRI system developed for research. It uses a permanent 1 Tesla magnet and a streamlined workflow to produce high-resolution images. Aspect Imaging's system is based on revolutionary permanent magnet technology. The magnet is highly efficient with no eddy currents from operation of the gradients. The system has high performance, silent gradients, highly sensitive RF coils, and powerful user-friendly application software providing high quality MR images. It includes a Personal Computer, an electronics cabinet, and a magnet sub-system.

2.4.1 Electronic cabinet

The electronics cabinet in (Figure 11) houses the following rack-mounted components:

a. The RF Amplifier that amplifies the Radio Frequency signal delivered by the RF coils.

b. The Control Unit that controls the Radio Frequency signal.
c. The Apollo Spectrometer that generates the pulse signals and captures the scan data.
d. The Gradient Amplifiers that amplify the gradient pulses.

The Power Distribution Unit (PDU) that distributes power to the system

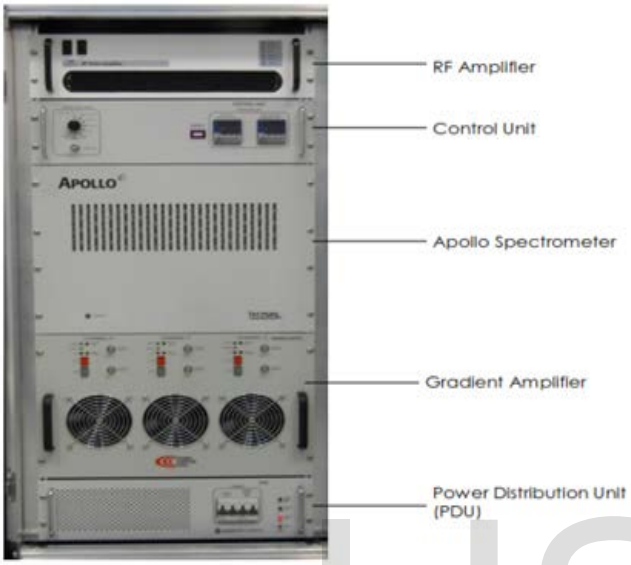

Figure 11: MRI Electronic Cabinet

2.4.2 Magnet Sub-system

The magnet assembly is a closed unit that is controlled by the Electronics Cabinet and the NRG Console software. In the front of the magnet assembly, located sample insertion opening or magnets bore. The coils (Figure 12) are calibrated to the required radio frequency for proton imaging and are used for RF transmission and reception. One of the coils is mounted in the back of the MRI magnet assembly at all times. For best quality of imaging, the smallest coil that will provide the tightest fit to the sample was used.

Coil A Coil B

Figure 12: Radio Frequency (RF) coils (A)is 35mm and (B) is 60mm coils

2.4.3 Positioning the Sample

Correct positioning of the sample is very important for obtaining high quality imaging results. Position the sample with the area of interest in the center of the RF coil and of the magnet. Make sure that the sample is positioned in the vertical center as well; if necessary, place it on top of a support as illustrated in (Figure 13). Place the sample in the Sample Handling unit, making sure that the area to be imaged is centered on the center mark.

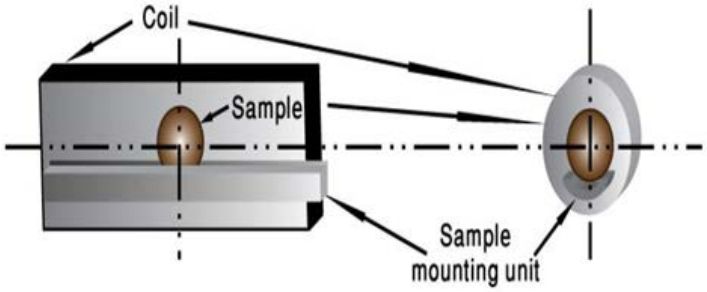

Figure 13: Sample Positioning in the Coil

2.4.4 Computer (PC)

The MRI system has a desktop PC and a 24" LCD monitor or console. The system software is comprised of three independent modules:

a. **NRG Console** is the main operation interface.
b. **NTNMR** is the instrument control, data acquisition, and data processing software program for the Tecmag Apollo spectrometer.
c. **Matlab** application constructs the MRI images from the raw data.

2.4.5 Data

The system scans the samples and generates raw data, which is reconstructed by the Matlab application into MRI images. The raw data file and images file format is 16-bit signed integer (least significant byte first). The raw data images and text files with all the parameters were stored in the system folder, **C:/program files/NRGSYS/NRGConsole/IMAGE/** for further off-line image processing. The folder contains folders for each image series, with a Dat file and image files for the series and all of its slices.

2.5 Operational Modes

The system includes three operational modes: Acquisition Mode, Edit Mode, and Design Mode. The display changes according to the selected mode.

Acquisition Mode: It is used for acquiring new images and is the most often used operating mode in routine operation. For this mode, (Figure 14) screen is display.

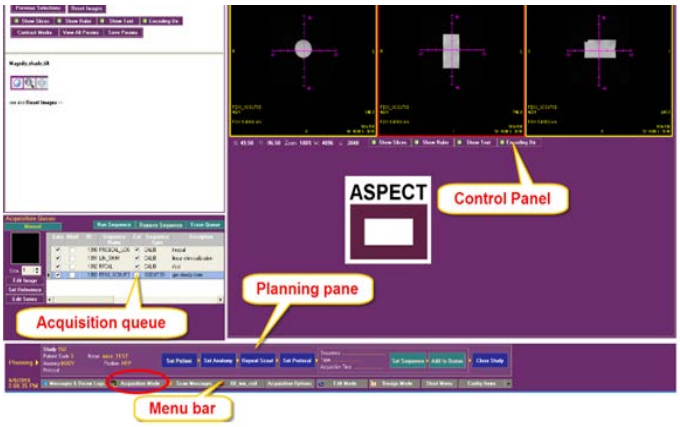

Figure 13: Acquisition Mode

Edit Mode: The Edit Mode is used for viewing and editing acquired images and series of images. When mode is selected, the system displays (Figure 15).

Figure 15: Edit Mode

Design Mode: The Design Mode is used for designing and modifying sequences and macros. When the mode is selected, the system displays (Figure 16).

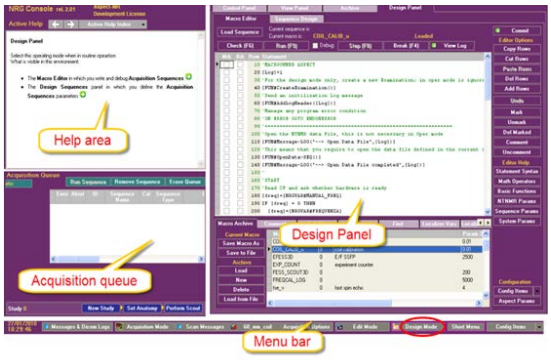

Figure 16: Design Mode

2.6 Verify RF Coil

In order to obtained best image quality, it was verified that the correct RF coil was identified by the system. The coil identification is displayed on a tab in the menu bar at the bottom of the screen (Figure 17).

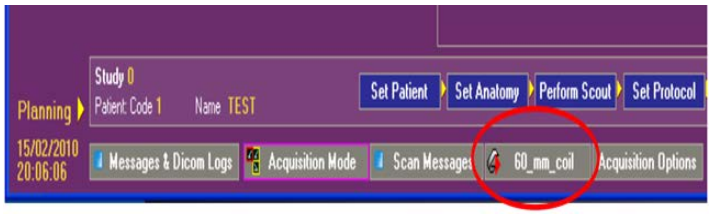

Figure 17: Menu bar

2.6.1 Magnetic resonance Instrumentation

The three important magnetic fields that are used to generate an MR image are listed in Table 2 and each of these components needs to be optimized to obtain reasonable data.

TABLE 2
List of three essential magnetic fields used in MRI

Types	Function
Strong magnet	Yields an external magnetic field $\mathbf{B_0}$
Radio Frequency resonator	Gives a $\mathbf{B_0}$ field for spin excitation and also used as the detector for image acquisition
Gradient coil set	Produces three orthogonal linear varying magnetic spatially fields, which are used for spatial encoding

2.6.2 Strong magnet

Various Magnetic Resonance Imaging systems have been developed in the last decades. The strength of the external magnetic fields currently used range from less than 0.5–21 T. There are merits as well as demerits associated with applying a high-field system. The advantages are the higher achievable equilibrium magnetisation $\boldsymbol{M_0}$ and a larger chemical shift. A higher $\boldsymbol{M_0}$ is equivalent to an increase in Signal to noise ratio (SNR) that is approximately linear with the magnetic field strength and can be used to increase either the spatial or the temporal resolution of the images. A larger chemical shift is particularly important in the fruit imaging of water-containing specimens.

The chemical shift between water and the fruit tissues resonances, e.g., in the soybean, is approximately 3.3 p.p.m. Although this chemical shift would result in a separation of only ~14 Hz at 0.1 T, a separation of ~1980 Hz is present at 14.1 T. Therefore, the suppression of water for object imaging at higher fields will be much easier.

The disadvantages of high field strengths are the significantly higher costs, limited available space within the bore of the magnet, and enhanced magnetic susceptibility effects arising from the inhomogeneity within samples. The use of high field magnets requires the use of liquid cryogens like liquid nitrogen and liquid helium to cool the superconductor. Ultra-high field systems usually have only a limited amount of sample space available. Bore sizes in the range of 5.4 cm at 20 T to 8.9 cm at 17.6 T are commercially available, but there are local-built systems with larger bore sizes. The enhanced susceptibility effects described occur because fruits are not homogeneous, and intracellular air spaces can produce susceptibility

artifacts. These rapid susceptibility changes produce local magnetic field gradients that disturb the homogenous $\mathbf{B_0}$ field. The result is a faster decay of the MR signal and thus a further reduction of T2. This reduced T2 is referred to as $T2^*$ and can be stated as :

$$1/\ 〚T2〛\ \hat{}\ * = 1/T2 + \gamma * \Delta B\_o \quad (12)$$

where γ is the gyromagnetic ratio and ΔB_0 is the difference in the strength of the locally varying field. Therefore, already short T2 times will become even shorter, which complicates the acquisition of the images. This effect increases with increasing field strength. Low-field (permanent or resistive) magnets have a number of advantages. These magnets are much less expensive and do not require cryogens for cooling.

In addition, some relatively lightweight versions are already available, such as the NMR-CUFF, which has field strength of 0.57 T and weighs only 3.1 kg (Raich & Blümler, 2004) Hence, it is possible to transport the system relatively easily for use in field experiments.

Another particular advantage of this magnet design is that the magnet can be opened and clamped around the object of interest, for instance a plant stem. Because the magnetic susceptibility effects at lower fields are much lower than those obtained at high magnetic fields, the resulting $T2^*$ time is longer. Experiments that cannot be conducted at high field strengths may be possible at lower field strengths. The disadvantages of low field magnets are the relatively low equilibrium magnetisation that can be achieved, the homogeneity of some of the magnets and the smaller chemical shift. Because the achievable $\boldsymbol{M_0}$ depends on the field strength, low-field magnets achieve limited resolution. Another problem with low-field transportable MRI systems can be the homogeneity of the B_0 field. Nevertheless, new designs can help to improve the homogeneity of B_0 (Windt, Soltner, Dusschoten, & Blümler, 2011)

2.6.3 Radio Frequency (RF) resonator

RF resonators are usually referred to as antennas that are used to produce the $\mathbf{B_1}$ field, which excites the spin system. Furthermore, these resonators are used to detect the response from the spin system. RF resonators can be divided in two classes:

i. Volume resonators ii. Surface resonators.

Volume resonators produce a very homogenous B_1 field. Their application is limited to the clear bore of their (usually) cylindrical geometry. These resonators can be used in fruits and seed imaging. Examples of volume resonators are:

a. Bird cage resonators b. TEM resonators c. Solenoids.

Solenoids have an opening that is perpendicular to the bore of the magnet. Thus, only samples of a limited length can be imaged using solenoids. Other resonators, such as the birdcage, have an opening that is parallel with the magnet bore, which allows the imaging of samples that are relatively long. Surface resonators have a less homogenous field than volume resonators and are thus used when only part of a fruits or plant needs to be imaged.

An example of surface resonators is a single loop surface resonator, which can be easily placed next to the farm produce region of interest (ROI). The sensitivity of these surface resonators is usually higher than that of a much larger volume resonator. It is important that the filling factor, which is the ratio of the sample volume to the total resonator volume, is relatively high. A low filling factor will result in a reduced signal to noise ratio (SNR).

2.6.4 Gradient

The spatial encoding of an MRI image is performed using three linear varying orthogonal magnetic fields that are created by the gradient set. Because of the limited space within the magnet, the gradient set should be as thin as possible. To create strong gradients, it is typically necessary to use circulating cooling water to remove the generated heat. These fields are switched very rapidly and can induce eddy currents in the system. Because these eddy currents can create image artifacts, special care has to be taken to alter the switching process of the gradients to compensate for the eddy current formation.

Commercially available systems have gradient strengths in the range of 0.2–1 T/m, whereas narrow-bore systems (magnet with a 5.4-cm bore diameter) can have strengths of up to 3 T/m.

The advantage of a stronger gradient set is the ability to make the necessary encoding faster and thereby reduce the echo time, which is the total elapsed time from the excitation to the acquisition of the data. This is particularly useful if images from resonances with short T2 or $T2^*$ are acquired. Furthermore, the use of a larger maximum gradient strength for image encoding in the frequency encoding direction will reduce the chemical shift artefact.

2.6.5 Storage

In the machine vision systems providing sufficient storage is usually a challenge since a single 8-bit image of 1024 x 1 024 pixels requires 1 Mb of storage. Digital data storage is of three types namely:

a. Archival storage.
b. On-line storage for relatively fast recall.
c. Short term storage use during processing.

Archival storage is characterized by massive storage requirement and magnetic disks and optical disks are used for such storage while for the short term storage, specialized boards or computer memory known as frame buffers are used and online storage generally takes the form of magnetic disks or visual memory. A Magneto-optical disk stores a terabyte of in-

formation.

2.6.6 Image Sensing and Acquisition

For this research work Magnetic Resonance Imaging systems were used for the purpose of internal quality farm produces image sensing and acquisition. The MRI image acquisition was performed with Aspect MRI equipment. The MRI system consists of hardware parts such as Electronics cabinet, Magnetic field gradient system, Permanent magnet, Radio-frequency system and Computer/Reconstruction system.

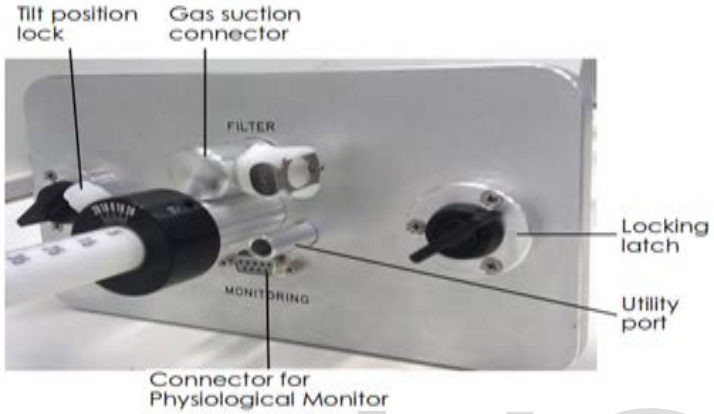

Figure 18: Face-plate of Sample Handling Unit

Each sample was placed on a plastic sample handling unit of (Figure 18) and position manually at the center such that the axis of the sample aligned with the center of the coil. During the alignment and de-alignment an emission and absorption of energy occurred in the RF of the electromagnetic. An image of the longitude slice was obtained along the axis of each sample specimens with different sequences.

Figure 19: Acquisition mode screen

Each sequence used was positioned such that all information on water proton is included in the MR image intensity and the pixels of each image were 128 x 128. The physical properties of the material such as relaxation time, temperature, density, flow, proton density and local differences in magnetic susceptibility determined the signal level of each voxel. MR images slides were acquired from MRI system using acquisition mode screen in (Figure 19)

TABLE 3
Basic MRI Terms (Balogun et al [20])

TERMS	MEANING
Spin	it is a fundamental part of nature like electrical charge which is in multiples of half (½) and can be positive or negative. Protons, electrons, and neutrons possess spin
Spin density	it is the density of mobile proton or the number of protons that posses enough mobility that can allow it to change direction and line up with the external magnetic field.
Larmor Frequency	is the precessional frequency when nuclear spin exhibit resonance
T_1 recovery	also known as longitudinal or Spin lattice relaxation time), is the recovery of magnetization along the axis of the external magnetic field B0. It is the period required for the 63% of the longitudinal magnetisation to recover in the tissue.
T_2 Decay	This is time constant characterizes the rate at which the M_{xy} component decays. It is caused by nuclei exchanging energy and defined as the period it takes 63% of the transverse magnetisation to be lost which is also known as spin-spin relaxation time.
Free Induction Decay Signal (FID)	This is the minimal voltage or signal 'S(t)' that is detected in the receiver coil due to the oscillating transverse component of the magnetisation after applying an RF pulse.
RF Coils	it produces the magnetic field B_1 which rotates the net magnetization in a pulse sequence. It also detects the transverse magnetization as it is precise in the XY plane. There are three types: transmit and receive coils, receive coils and transmit coils only.
Resonance	This occurs when the radio frequency pulse equals the frequency of precession of the protons

3.0 CONCLUSION AND FUTURE WORK

The main focus of this research work is to illustrate the proposed operational concept of acquiring magnetic resonance image of farm produce. The main component of magnetic resonance imaging which comprises a Personal Computer, an electronics cabinet, and a magnet sub-system were illustrated and discussed. The theoretical background of this component was further discussed and evaluated theoretically and practically.

This work shows steps of acquiring images in MRI machine and possibility of developing portable MRI machine for agricultural experimental field work which may result into usage of coupling portable MRI machine with robot or unmanned aerial vehicle (UAV)/drone for online assessment of internal quality of farm produce as it develop or grow in the farm field.

REFERENCES

[1] Kondo, N. (2010). Automation on fruit and vegetable grading system and food traceability. *Trends in Food Science & Technology, 21*(3), pp. 145-152.

[2] Du, C.-J., & Sun, D.-W. (2004). Recent developments in the applications of image processing techniques for food quality evaluation. *Trends in Food Science & Technology, 15*(5), pp. 230-249.

[3] Kleynen, O., Leemans, V., & Destain, M.-F. (2005). Development of a multi-spectral vision system for the detection of defects on apples. *Journal of Food Engineering, 69*(1), pp. 41-49.

[4] Ebrahimnejad, H., Ebrahimnejad, H., Salajegheh, A., & Barghi, H. (2018). *Use of Magnetic Resonance Imaging in Food Quality Control: A Review* (Vol. 8) journal of Biomed Phys Eng

[5] Zhang, L., & McCarthy, M. J. (2012). Measurement and evaluation of tomato maturity using magnetic resonance imaging. *Postharvest Biology and Technology, 67*(0),pp.37-43.doi: http://dx.doi.org/10.1016/j.postharvbio.2011.12.004

[6] Bhaiya, L. P., & Verma, V. K. (2012). Classification of MRI Brain Images Using Neural Network. *network, 2*(5), pp. 751-756.

[7] Pekar, J. J. (2006). A brief introduction to functional MRI.*Engineering in Medicine and Biology Magazine, IEEE, 25*(2), pp. 24-26.

[8] Euclid Seeram Prize for CT and MRI pioneers Australian Institute of Radiography The Radiographer 2006: 53 (1): 4–7

[9] Nishimura, D. G. (1996). *Principles of magnetic resonance imaging*: Stanford University.

[10] Hashemi, R. H., Bradley, W. G., & Lisanti, C. J. (2010). *MRI: the basics*: Lippincott Williams & Wilkins.

[11] Hornak, J. P. (2007). The Basics of MRI (1996). *Web book available at http://www. cis. rit. edu/htbooks/mri/. Accessed July, 17*.

[12] Talagala, S. L., & Lowe, I. J. (1991). Introduction to magnetic resonance imaging. *Concepts in Magnetic Resonance, 3*(3), pp. 145-159.

[13] Yang, J., Feng, C., & Zhao, D. (2012). A CUDA-based reverse gridding algorithm for MR reconstruction. *Magnetic resonance imaging*.

[14] Hinshaw, W. S., & Lent, A. H. (1983). An introduction to NMR imaging: From the Bloch equation to the imaging equation. *Proceedings of the IEEE, 71*(3), pp. 338-350.

[15] Zhang, L., & McCarthy, M. J. (2013). Assessment of pomegranate postharvest quality using nuclear magnetic resonance. *Postharvest Biology and Technology, 77*, pp. 59-66.

[16] Edelstein, W., Hutchison, J., Johnson, G., & Redpath, T. (1980). Spin warp NMR imaging and applications to human whole-body imaging. *Physics in medicine and biology, 25*(4), pp. 751.

[17] Westbrook, C., & Roth, C. K. (2013). *MRI in Practice*: Wiley-Blackwell.

[18] Li, T.-Q., Ödberg, L., Powell, R. L., & McCarthy, M. J. (1995). Quantitative measurements of flow acceleration by means of nuclear magnetic resonance imaging. *Journal of Magnetic Resonance, Series B, 109*(2), pp. 213-217.

[19] Aibinu, A. M., Salami, M. J. E., Shafie, A. A., & Najeeb, A. R. (2008). MRI reconstruction using discrete fourier transform: a tutorial.

[20] Balogun W.A. Momoh-Jimoh E. Salami, M. J. McCarthy, Y. M. Mustafah, A. M. Aibinu (2013) *Intelligent Technique for Grading Tropical Fruit using Magnetic Resonance Imaging* International Journal of Scientific & Engineering Research, 4(7) pp216-225

.